Staggered Fermions and Gauge Field Topology

P.H. Damgaard[a], U.M. Heller[b], R. Niclasen[a] and K. Rummukainen[c,d]

[a]The Niels Bohr Institute and [c]NORDITA
Blegdamsvej 17
DK-2100 Copenhagen, Denmark

[b]SCRI
Florida State University
Tallahassee, FL 32306-4130, USA

[d]Helsinki Institute of Physics,
P.O.Box 9, 00014 University of Helsinki, Finland

February 1, 2008

Abstract

Based on a large number of smearing steps, we classify SU(3) gauge field configurations in different topological sectors. For each sector we compare the exact analytical predictions for the microscopic Dirac operator spectrum of quenched staggered fermions. In all sectors we find perfect agreement with the predictions for the sector of topological charge zero, showing explicitly that the smallest Dirac operator eigenvalues of staggered fermions at presently realistic lattice couplings are insensitive to gauge field topology. On the smeared configurations, 4ν eigenvalues clearly separate out from the rest on configurations of topological charge ν, and move towards zero in agreement with the index theorem.

1   Introduction

The study of the relation between staggered fermions and (lattice) gauge field topology has a long history, beginning with the work of Smit and Vink [1]. In particular, it is well known that staggered fermions at realistic values of the gauge field coupling β do not show the proper relation between fermion zero modes and gauge field topology as it is dictated by the index theorem in the continuum. This established problem with staggered fermions has recently surfaced again, as lattice gauge theory studies have begun to test in detail the exact analytical predictions for the microscopic Dirac operator spectrum of staggered fermions [2, 3, 4, 5]. The crucial point is that the whole microscopic Dirac operator spectrum, and not just that pertaining to the exact zero modes, has been predicted to be very strongly dependent on the gauge field topology [6]. It falls into one of a set of universality classes that in addition depend on the gauge group, the number of fermion flavors and their color representation [7, 8, 9, 10].

In earlier studies [2, 3, 4, 5] of the spectrum of the smallest staggered Dirac operator eigenvalues *all* gauge field configurations, irrespective of their possibly non-trivial winding numbers, were simply bunched together, and the Dirac operator spectrum taken with respect to this full average. This implies an implicit sum over all topological sectors, for which the analytical predictions are very different from those of sectors with fixed topological index [11]. Nevertheless, absolutely excellent agreement was found when comparing with just the sector of vanishing topological charge $\nu = 0$. On the surface this may seem to be just a simple consequence of the fact that also exact zero fermion modes are missing in the staggered formulation. The issue is, however, much more complicated. The lattice studies of refs. [2, 3, 4, 5] involved the distribution of just around 10 of the lowest Dirac operator eigenvalues. Only positive eigenvalues were considered, since the staggered Dirac spectrum has an exactly $\pm$ symmetric spectrum. Of these few lowest eigenvalues, typically one would expect that up to 2-6 were actually the "would-be" zero modes, shifted away from the origin by the staggered fermion artefacts. What should be the distribution of these "wrong" small eigenvalues? In the Random Matrix Theory formulation of the problem [7, 8] there is no answer to this question, as there is no known way of imposing correctly almost-zero modes in the theory. In that formulation one either *has* or *has not* exact zero eigenvalues. This could incorrectly lead to the conclusion that as long as staggered fermions do not produce *exact* zero modes, the distribution of the smallest Dirac operator eigenvalues in that formulation will exactly equal that of the $\nu = 0$ sector. The argument is false, because as β is increased the appropriate number of the smallest Dirac operator eigenvalues will slowly separate out, and move towards the origin. As this happens, the whole microscopic Dirac operator spectrum will continuously shift, and in this intermediate region there will certainly no longer be agreement with the analytical predictions for *any* sectors with $\nu \neq 0$, let alone the sum over all of them.

These considerations immediately raise the question of whether already at the β-values considered in refs. [2, 3, 4, 5] there was appreciable contamination of "wrong" non-zero eigenmodes. To settle that issue, we report here on a high-statistics analysis (involving around 17,000 gauge field configurations) of the microscopic Dirac operator spectrum of SU(3) gauge theory with quenched staggered fermions. Correctly classifying the gauge field configurations according to topology is not a simple task, especially since by default we are excluded from using fermionic methods. We have chosen to do the classification according to the result of measuring the naive latticized topological charge

$$\nu \;=\; \frac{1}{32\pi^2} \int d^4 x \mathrm{Tr}[F_{\mu\nu} F_{\rho\sigma}]\epsilon_{\mu\nu\rho\sigma} \tag{1}$$

on configurations obtained after a large number of so-called APE smearing steps [12], details of which will be given below. Once classified, we have then measured the smallest Dirac operator eigenvalues

on the original *un-smeared* gauge field configurations. We in no way claim that this is an optimal way in which to separate out the different topological sectors, but it should at least have quite some overlap with other methods. In particular, it is known, on average, to produce results very similar to more conventional types of semi-classical cooling [13].

Studying the fate of the smallest Dirac operator eigenvalues with staggered fermions is here motivated by the need to understand the exact analytical predictions for the microscopic Dirac operator spectrum. But the problem is interesting also for other reasons. For instance, one needs to know the extent to which staggered fermions correctly couple to gauge field topology also if one wishes to compute, for instance, flavor singlet pseudoscalar masses in lattice QCD. We believe that the microscopic Dirac operator spectrum may be an excellent tool with which to assess how close simulations with staggered fermions are to continuum physics related to gauge field topology and the anomaly.

This short paper is organized as follows. In the next section we briefly describe how we implement the smearing technique on gauge links, and show how this leads us to a classification of all gauge field configurations into distinct sectors, labelled by the value of ν. We also trace the evolution of the smallest Dirac operator eigenvalues as a function of the number of smearing steps, and show that these results are completely in accord with expectations. In section 3 we compute the microscopic Dirac operator spectrum in each of the different gauge field sectors, and compare results to the analytical predictions. To zoom in on precisely the *smallest* eigenvalue, which in topologically non-trivial sectors should behave very differently from the ordinary Dirac operator eigenvalues, we also compare the distribution of just this smallest eigenvalue with the exact analytical predictions. Finally, section 4 contains our conclusions.

2 Analysis of Gauge Field Topology: APE-Smearing

We perform the statistical analysis of the gauge field topology and the Dirac operator eigenvalues using a total of 17454 SU(3) pure gauge configurations with volume $V = 8^4$ and lattice coupling $\beta = 6/g^2 = 5.1$. We generate the configurations with an update consisting of 4 microcanonical overrelaxation sweeps over the volume followed by one pseudo–heat-bath update. The configurations we analyze are separated by 20 of these compound sweeps; this guarantees that the configurations are effectively uncorrelated.

Let us give some technical details about the measurements of the topological charge. First, the naive topological density operator (1), when implemented on the lattice, is not truly topological: it is sensitive to lattice ultraviolet modes, and, if applied to the original lattice configurations, the (generally non-integer) value of ν is completely dominated by the UV noise. However, if the fields are smooth enough on the lattice scale, topology can be uniquely defined.

We make the original lattice fields smoother by applying repeated APE-smearing: during one smearing sweep, SU(3) link variables $U_\mu(x)$ are replaced by

$$U_\mu(x) \to P_{\mathrm{SU}(3)} \left[f U_\mu(x) + \sum_{|\nu| \neq \mu} U_\nu(x) U_\mu(x+\nu) U_\nu^\dagger(x+\mu) \right], \qquad (2)$$

where the sum over ν goes over both positive and negative directions. The operator $P_{\mathrm{SU}(3)}$ projects the $3{\times}3$ complex matrix $W_\mu(x)$, inside the brackets in (2), to SU(3), and f is an adjustable parameter.
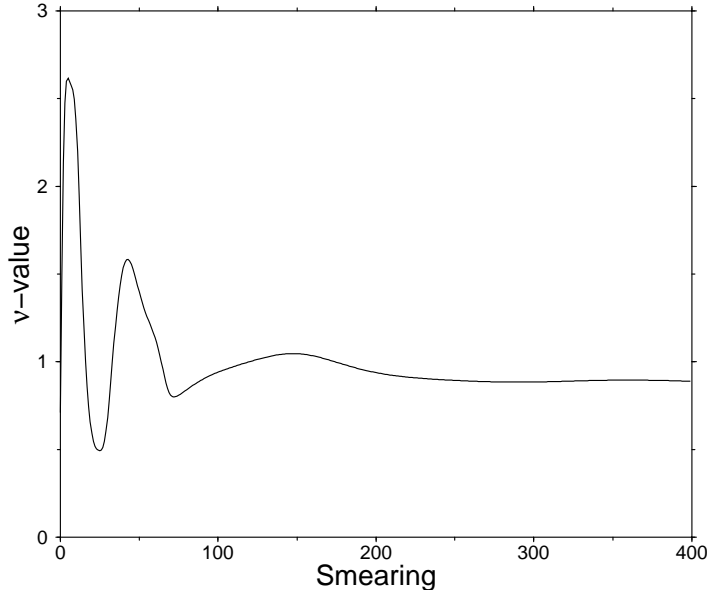
Figure 1: The topological charge of one configuration, measured during the APE-smearing. After initial 'noise,' the charge measurement quickly stabilizes to an almost-integer value.

The projection is performed by maximizing $\mathrm{Tr}\left(U'_\mu(x)W^\dagger_\mu(x)\right)$ over the SU(3) group elements $U'_\mu(x)$. The smearing sweeps (consisting of a smearing of each link on the lattice) are performed up to 400 times.

While the APE-smearing is not particularly sensitive to the actual choice of the parameter f, we used $f = 7$ throughout our work. This value is motivated by the comparison to the RG blocking analysis by De Grand *et al* [13]. According to their results, APE-smearing is quite effective in resolving instantons from quantum fluctuations, while it preserves the long-distance properties of the gauge field configurations much better than the standard cooling algorithms. Naturally, almost any cooling or smearing method will destroy instantons with a size of order of the lattice spacing; however, the lattice topology is not well defined at these length scales anyway.

We calculate the field tensor $F_{\mu\nu}$ in Eq. (1) at lattice point x by symmetrizing over the 'clover' of the 4 (μ, ν)-plane plaquettes which have one corner at point x. In Fig. 1 we show a typical example of how the topological charge (as measured with operator (1)) develops during smearing. As expected, the charge measurement is very noisy when the configurations are rough, but after ~ 100 smearing sweeps the measurement almost always stabilizes to almost an integer value, which is then preserved for at least several hundreds of smearing steps.

In Fig. 2 we show the distribution of the measured topological charge after 200 smearing steps. The distribution is strongly peaked near integer values, as expected, with a small downward drift of the peaks from exact integer values. This is obviously caused by our naive $F\tilde{F}$ operator; using an improved operator would presumably shift the peaks toward exact integer values. Nevertheless, this slight shift does not pose any difficulties in assigning a topological index to the smeared configurations. Indeed, it is fairly obvious from our figure that there is simply a trivial "renormalization" of the naive topological charge, which appears to be neatly quantized, not in units of integers, but in units of around ~ 0.8. If corrected with such a prefactor of $\sim 1/0.8$, our distribution of topological charges will fall on values
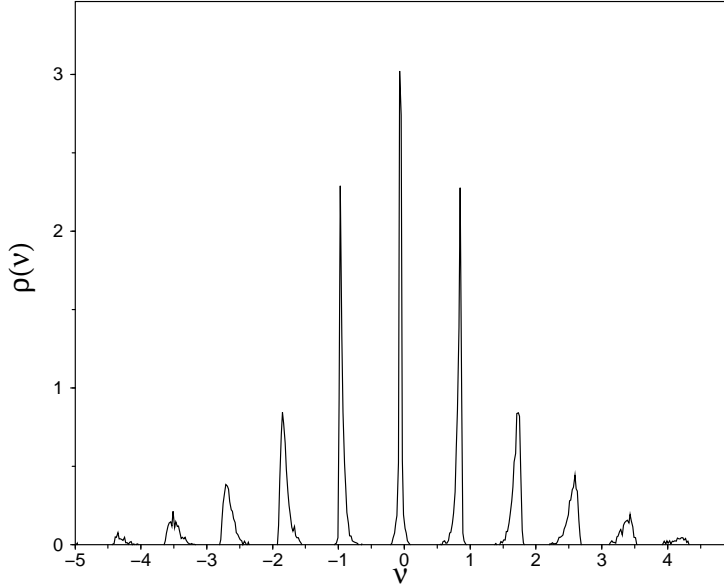
3

Figure 2: The distribution of the topological charge, measured from 17454 $V = 8^4$, $\beta = 5.1$ configurations.

very close to integers, and, as seen, the distribution has the expected infinite-volume Gaussian shape.

We have measured the topological charge after 200 and 300 smearing sweeps, and accepted only configurations where the measured charge remained in the neighborhood of the same "renormalized" integer value $0, \pm 1, \pm 2$. In this way we have rejected configurations where the measured topological charge changed too much to be uniquely defined. In this process we have rejected 37% of our configurations, which simply have been discarded in all of the subsequent analysis.

Eigenvalues of the staggered Dirac operator

$$
\begin{aligned}
\displaystyle \not{D}_{x,y} &= \frac{1}{2}\sum_{\mu} \eta_\mu(x)\left(U_\mu(x)\delta_{x+\mu,y} - U_\mu^\dagger(y)\delta_{x,y+\mu}\right) \\
&\equiv \not{D}_{e,o} + \not{D}_{o,e}
\end{aligned}
\tag{3}
$$

are computed using the variational Ritz functional method [14]. Here $\eta_\mu(x) = (-1)^{\sum_{\nu < \mu} x_\nu}$ are the staggered phase factors. Letting $\epsilon(x) = (-1)^{\sum_\nu x_\nu}$, we have explicitly indicated how $\not{D}$ connects *even* sites, i.e. those with $\epsilon(x) = +1$, with *odd* (those with $\epsilon(x) = -1$) ones, and vice versa. We remind the reader that the staggered Dirac operator is antihermitian with purely imaginary eigenvalues that come in pairs, $\pm i\lambda$. The operator $-\not{D}^2$ is thus hermitian and positive semi-definite, and the sign function $\epsilon(x)$ defined above plays the role of γ_5 in the continuum (*i.e.*, this quantity anticommutes with $\not{D}$: $\{\not{D}, \epsilon\} = 0$). Moreover, since $-\not{D}^2$ does not mix between even and odd lattice sites, it suffices to compute the eigenvalues, on, say, the even sublattice. In fact, if ψ_e is a normalized eigenvector of $-\not{D}^2$ with eigenvalue λ^2, then $\psi_o \equiv \frac{1}{\lambda}\not{D}_{o,e}\psi_e$ is a normalized eigenvector of $-\not{D}^2$ with eigenvalue λ^2, and non-zero only on odd sites. (Note that there is no difficulty with the above definition of ψ_o, since we will never encounter exact zero modes). In practice, we make use of these properties, and compute only the (positive) eigenvalues of $-\not{D}^2$ restricted to the even sublattice, and then take the (positive) square root. All eigenvalues to be shown in the following thus have an equal number of negative companions, of the exact same magnitude.
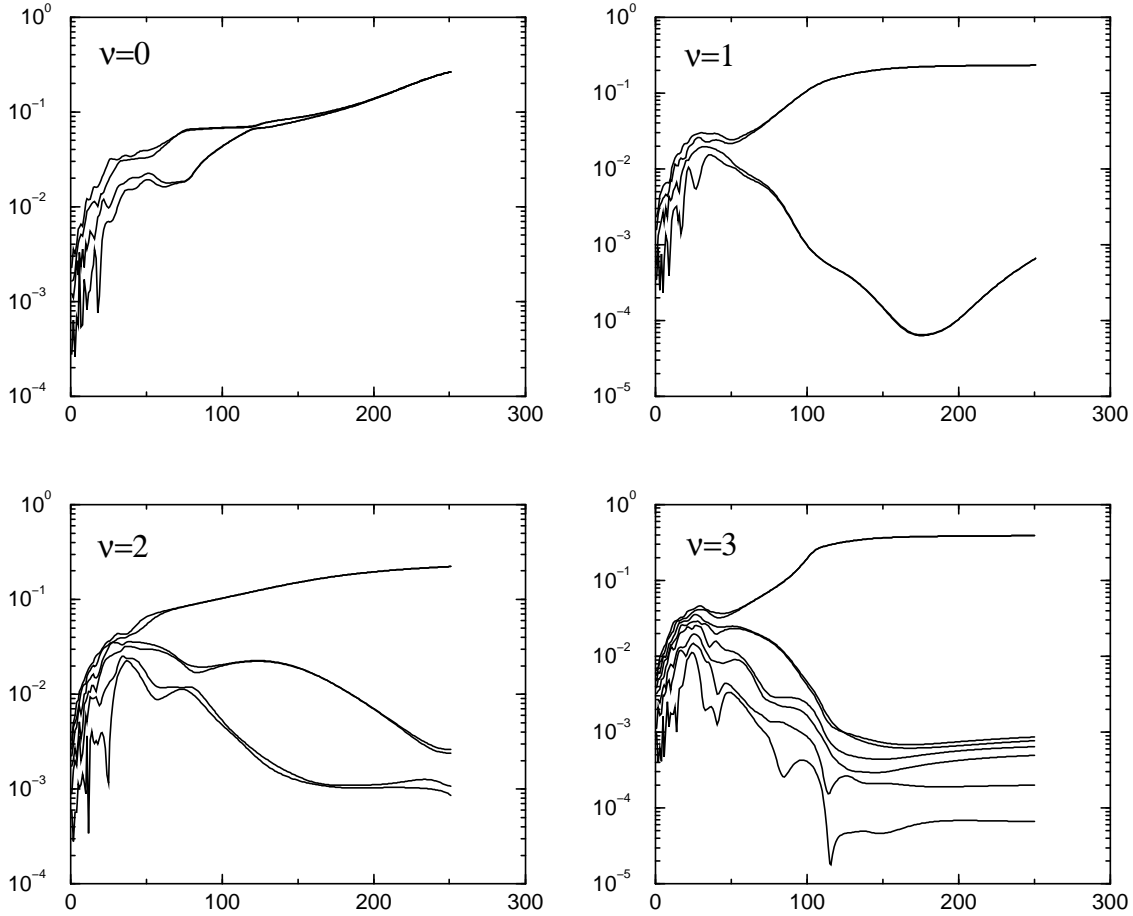
4

Figure 3: The behaviour of the lowest Dirac operator eigenvalues during the APE smearing. In each case there are $4 \times \nu$ small eigenvalues; only the positive eigenvalues are shown here.

We have first investigated how the lowest eigenvalues behave during the smearing process described previously. As shown in Fig. 3, the index theorem is seen to be valid for smooth configurations: after ~ 100 smearing sweeps, we have exactly $4 \times \nu$ very small eigenvalues (corresponding to 4 continuum flavors for each staggered fermion flavor), whereas the other eigenvalues grow larger. This implies that in the continuum limit the eigenvalues of the staggered Dirac operator should indeed depend on the topology of the gauge configuration. As expected, on the smooth configurations the counting of flavors is precisely as in the continuum limit: we observe 4 flavor degrees of freedom associated with the staggered Dirac operator.

3   The Microscopic Dirac Operator Spectrum

Having described our procedure for classifying our gauge field configurations according to their smeared topological charge ν, we now proceed to measure the distribution of the smallest Dirac operator eigenvalues. We stress that we use the smearing technique *only* as a means of defining the classification of the original un-smeared gauge field configurations. All measurements presented below are performed on the original, *un-smeared*, gauge field configurations, after having discarded those that failed to be classified according to the criterion described above.

The spectral density of the Dirac operator is given by

$$\rho^{(\nu)}(\lambda) \equiv \left\langle \sum_n \delta(\lambda - \lambda_n) \right\rangle_\nu \tag{4}$$

in each sector of topological charge ν. The associated microscopic Dirac operator spectrum is defined by enhancing the smallest eigenvalues according to the size of the lattice space-time volume V. Let

$$\Sigma = \lim_{m \to 0} \lim_{V \to \infty} \langle \bar{\psi}\psi \rangle \tag{5}$$

denote the infinite-volume chiral condensate as defined in the conventional manner. One then blows up the small eigenvalues by keeping $\zeta \equiv \lambda \Sigma V$ fixed as $V \to \infty$, and introduces the microscopic spectral density [7]

$$\rho_s^{(\nu)}(\zeta) \equiv \frac{1}{V} \rho^{(\nu)}\left(\frac{\zeta}{\Sigma V}\right) , \tag{6}$$

which then again is measured in each topological sector. For the case at hand, the microscopic spectral density has been computed from both Random Matrix Theory [7] and from the effective finite-volume partition functions [9, 10]. The results agree, and the simple analytical result for the quenched theory ($J_n(x)$ is the nth order Bessel function),

$$\rho_s^{(\nu)}(\zeta) = \pi\rho(0)\frac{\zeta}{2}\left[J_\nu(\zeta)^2 + J_{\nu-1}(\zeta)J_{\nu+1}(\zeta)\right] \tag{7}$$

is exact in the limit where $V \to \infty$ and $V \ll 1/m_\pi^4$. Here $\rho(0)$ is the macroscopic spectral density of the Dirac operator, evaluated at the origin. By the well-known Banks-Casher relation, it is related to the chiral condensate through $\pi\rho(0) = \Sigma$.

In Fig. 4 we compare these analytical predictions for the sectors of $\nu = 0, 1$ and 2. We did not have enough statistics to perform a similar analysis on what we would classify as $\nu = 3$ configurations; however, as will be evident, there was no need to do this either. Our first comment concerns statistics. Because the configurations with $+\nu$ and $-\nu$ should give rise to the same microscopic Dirac operator spectrum, we actually end up with better statistics for the $\nu = \pm 1$ configurations combined. In total, we had 2683 configurations labelled as $\nu = 0$, 4797 configurations labelled as $\nu = \pm 1$, and 3493 configurations labelled as $\nu = \pm 2$. Indeed, we observe from Fig. 4 the curious fact that the agreement between the analytical curve for the microscopic spectral density of the staggered Dirac operator actually seems to be poorer on the $\nu = 0$ than on the $\nu = \pm 1$ configurations. We attribute this solely to statistical fluctuations. It is quite obvious that even configurations classified as of $\nu = \pm 1$ and $\nu = \pm 2$ topological charge give rise to a microscopic staggered Dirac operator spectrum here which is indistinguishable from that of the $\nu = 0$ configurations. The agreement with the exact analytical formula for $\nu = 0$ configurations (7) is extraordinarily good on all three classes of configurations. We have also indicated on the figure the predictions for $|\nu| = 1$ and $|\nu| = 2$; there is clearly no way our Monte Carlo data can be compatible with these predictions. Combining all data, we obtain perfect agreement with the analytical $\nu = 0$ prediction, with very small statistical errors.

To focus more closely on just the smallest eigenvalue, we have also compared its distribution with the analytical predictions for different topological sectors [15]. Let us denote the distribution of the lowest (rescaled) eigenvalue in a sector of topological charge ν by $P^{(\nu)}(\zeta)$. From the general formula of ref. [15] one finds for the quenched theory, with our normalization convention:

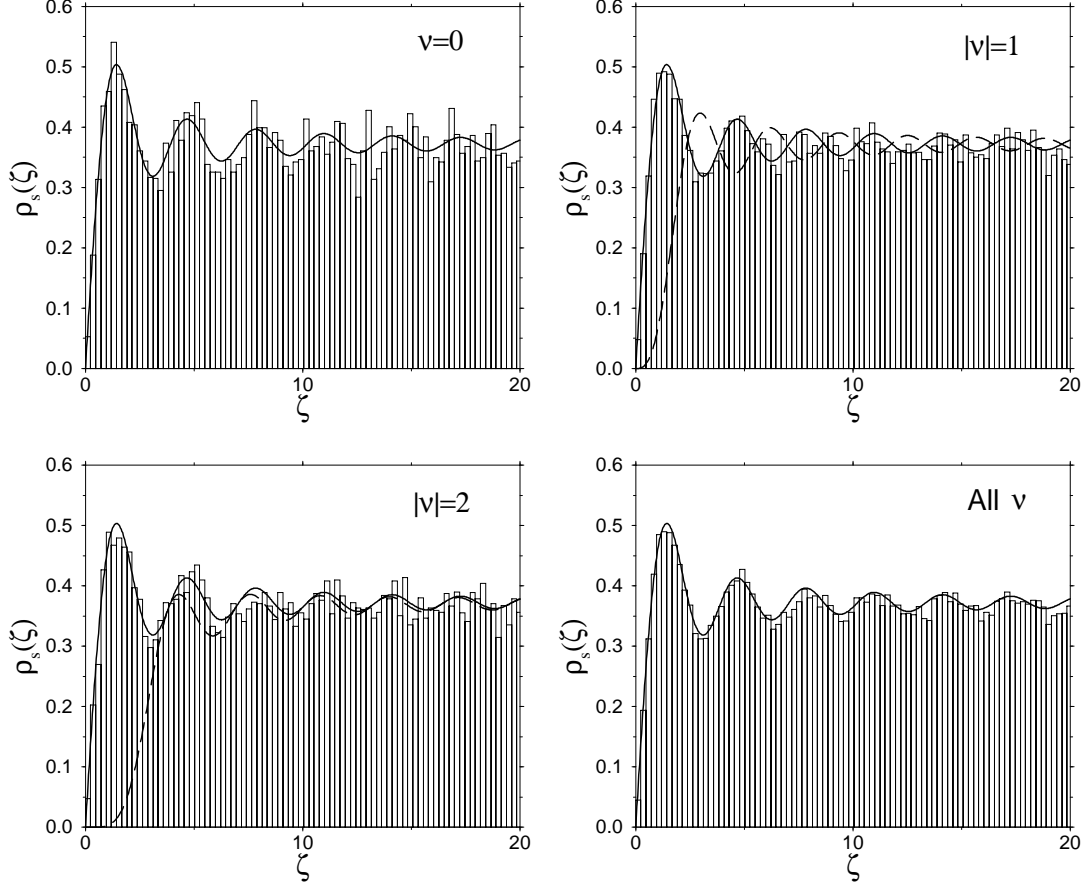$$P^{(0)}(\zeta) = \pi\rho(0)\frac{\zeta}{2}e^{-\zeta^2/4}$$

6

Figure 4: The microscopic spectral density of the Dirac operator for topological sectors $\nu = 0$, 1 and 2, and for all of the configurations combined. The continuous line is the theoretical prediction for the sector $\nu = 0$, and the dashed lines are the predictions for $|\nu| = 1$ and 2.

$$
\begin{aligned}
P^{(1)}(\zeta) &= \pi\rho(0)\frac{\zeta}{2}I_2(\zeta)e^{-\zeta^2/4} \\
P^{(2)}(\zeta) &= \pi\rho(0)\frac{\zeta}{2}\left[I_2(\zeta)^2 - I_1(\zeta)I_3(\zeta)\right]e^{-\zeta^2/4} .
\end{aligned}
\tag{8}
$$

Checking the distribution of just the smallest eigenvalue is obviously the most sensitive test of whether there is any appreciable contamination of would-be zero modes in the different topological sectors. We show in Fig. 5 the lowest eigenvalue distributions in the three different topological sectors, and compare them with the analytical predictions. Clearly no deviations are seen at all from the $\nu = 0$ prediction, in all sectors.

Finally, one could well ask what would happen if we instead measured the distribution of the smallest staggered Dirac operator eigenvalues on the *smeared* configurations, after removing by hand those eigenvalues that obviously should be classified as zero modes. All indications are of course that such smeared configurations should produce the correct behavior of the eigenvalues in the different topological sectors. The reason why we have not performed such measurements on the smoothened configurations is that the ensemble average is not a very meaningful concept in that case. The results are clearly very sensitive to where we cut the APE-smearing procedure, and even with a fixed number
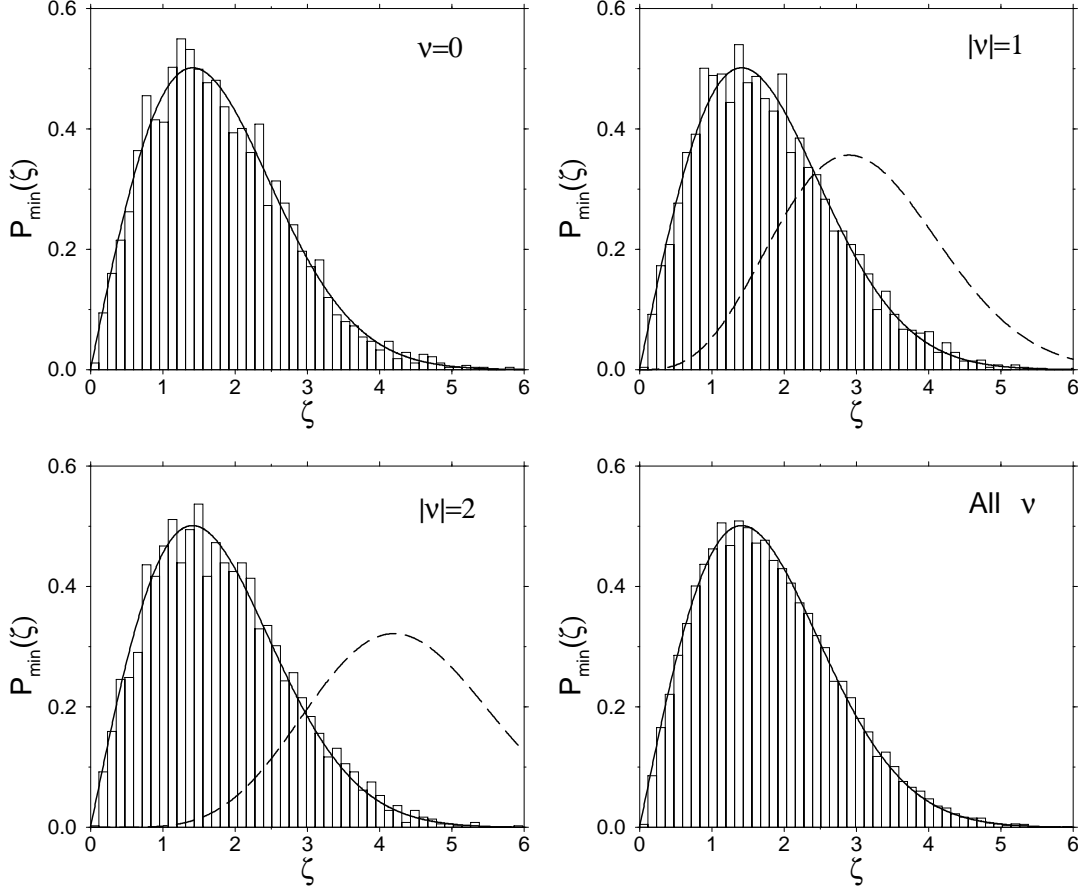
7

Figure 5: The distribution of the lowest eigenvalue of the Dirac operator for topological sectors $\nu = 0$, 1, 2, and for the sum over all configurations. Continuous (dashed) lines show the theoretical prediction for $\nu = 0$ ($|\nu| = 1, 2$).

of smearings it is not at all obvious that this could provide us with a sensible ensemble average.

4 Conclusions

At a lattice coupling of $\beta = 5.1$ the microscopic Dirac operator spectrum of staggered fermions in quenched SU(3) lattice gauge theory displays *no deviations at all* from the analytical prediction of the $\nu = 0$ topological sector. Even after roughly classifying all gauge field configurations into different topological sectors by means of the value of $F\tilde{F}$ on sufficiently smeared configurations, we have found no deviations from the $\nu = 0$ predictions, in any of the different sectors. In view of earlier results, which simply bunched all gauge field configurations together independently of their proper assignments of topological charge [2, 3, 4, 5], and which found excellent agreement on this total sample of configurations, these results are not extremely surprising. It is nevertheless very disturbing that at the presently probed lattice couplings even gauge field configurations that clearly should be classified as carrying non-trivial topological charge ν are not at all seen as such by staggered fermions. The agreement with the analytical predictions for the microscopic Dirac operator spectrum in a gauge field sector of topological charge zero is thus a great success of the analytical framework [7, 8, 9, 10], but it also indicates a clear failure of the staggered fermion formulation at these lattice couplings. What it

8

means is that Monte Carlo simulations with staggered fermions at these lattice couplings are oblivious to net gauge field topology, an essential ingredient of the dynamics of non-Abelian gauge theories. Such simulations are simply not mimicking the correct path integral of the continuum theory. It is comforting that more sophisticated fermion formulations that correctly build in the broken/unbroken chiral Ward identities in sectors of fixed gauge field topology now are feasible alternatives. There are already clear results which show that these new fermion formulations correctly reproduce the analytical predictions for the microscopic Dirac operator spectrum in sectors of non-trivial gauge field topology [16, 17, 18].

One surprising aspect of the present work is that it shows that the typically 2-6 would-be zero modes of staggered fermions at these lattice spacings behave entirely as "conventional" (small) Dirac operator eigenvalues on topologically trivial configurations. In particular, although they consist of up to 50% of all the small eigenvalues we probe here, their distributions fall entirely on top of the conventional small eigenvalues. Certainly, these would-be zero modes will eventually, as the lattice spacing is decreased, separate out, and completely distort the microscopic Dirac operator spectrum. This deformation of the smallest eigenvalue spectrum may already have been seen in the 2-d Schwinger model [19]. It is challenging to search for the corresponding onset of correct topological properties with staggered fermions in this SU(3) gauge theory at smaller lattice spacings. The microscopic Dirac operator spectrum is an excellent tool with which to measure this in a precise and quantitative manner.

References

[1] J. Smit and J.C. Vink, Nucl. Phys. **B286** (1987) 485; Nucl. Phys. **B298** (1988) 557; Nucl. Phys. **B303** (1988) 36.
J.C. Vink, Nucl. Phys. **B307** (1988) 549; Phys. Lett. **212B** (1988) 483.

[2] J.J.M. Verbaarschot, Phys. Lett. **B368** (1996) 137.

[3] M.E. Berbenni-Bitsch, S. Meyer, A. Schäfer, J.J.M. Verbaarschot and T. Wettig, Phys. Rev. Lett. **80** (1998) 1146.
M.E. Berbenni-Bitsch, S. Meyer, T. Wettig, Phys. Rev. **D58** (1998) 071502.

[4] P.H. Damgaard, U.M. Heller and A. Krasnitz, Phys. Lett. **B445** (1999) 366.
M. Göckeler, H. Hehl, P.E.L. Rakow, A. Schäfer and T. Wettig, Phys. Rev. **D59** (1999) 094503.

[5] R.G. Edwards, U.M. Heller and R. Narayanan, hep-lat/9902021.

[6] J. Gasser and H. Leutwyler, Phys. Lett. **188B** (1987) 477.
H. Leutwyler and A. Smilga, Phys. Rev. **D46** (1992) 5607.

[7] E.V. Shuryak and J.J.M. Verbaarschot, Nucl. Phys. **A560** (1993) 306.
J.J.M. Verbaarschot and I. Zahed, Phys. Rev. Lett. **70** (1993) 3852.

J.J.M. Verbaarschot, Phys. Lett. **B329** (1994) 351; Nucl. Phys. **B426** (1994) 559; Phys. Rev. Lett. **72** (1994) 2531.

[8] G. Akemann, P.H. Damgaard, U. Magnea and S. Nishigaki, Nucl. Phys. **B487** (1997) 721.
P.H. Damgaard and S.M. Nishigaki, Nucl. Phys. **B518** (1998) 495.
M.K. Şener and J.J.M. Verbaarschot, Phys. Rev. Lett. **81** (1998) 248.

[9] P.H. Damgaard, Phys. Lett. **B424** (1998)322.
G. Akemann and P.H. Damgaard, Nucl. Phys. **B519** (1998) 682; Phys. Lett. **B432** (1998) 390.

[10] J.C. Osborn, D. Toublan and J.J.M. Verbaarschot, Nucl. Phys. **B540** (1998) 317.
P.H. Damgaard, J.C. Osborn, D. Toublan and J.J.M. Verbaarschot, Nucl. Phys. **B547** (1999) 305.
D. Toublan and J.J.M. Verbaarschot, hep-th/9904199.

[11] P.H. Damgaard, hep-th/9903096.

[12] M. Falcioni, M. Paciello, G. Parisi, B. Taglienti, Nucl. Phys. **B251**[FS13] (1985) 624.
M. Albanese et al., Phys. Lett. **B192** (1987) 163.

[13] T. DeGrand, A. Hasenfratz and T.G. Kovacs, Nucl. Phys. **B505** (1997) 417; Nucl. Phys. **B520** (1998) 301.

[14] B. Bunk, K. Jansen, M. Lüscher, H. Simma, DESY report Sept. 1994; T. Kalkreuter and H. Simma, Comp. Phys. Comm. **93** (1996) 33.

[15] S.M. Nishigaki, P.H. Damgaard and T. Wettig, Phys. Rev. **D58** (1998) 087704.

[16] F. Farchioni, I. Hip, C.B. Lang and M. Wohlgenannt, Nucl. Phys. **B549** (1999) 364.

[17] R.G. Edwards, U.M Heller, J. Kiskis and R. Narayanan, Phys. Rev. Lett. **82** (1999) 4188.

[18] P.H. Damgaard, R.G. Edwards, U.M. Heller and R. Narayanan, hep-lat/9907016.

[19] F. Farchioni, I. Hip and C.B. Lang, hep-lat/9907011.